

# Surface Dean–Kawasaki equations

John Bell<sup>1</sup>, Ana Djurdjevac<sup>2</sup>, and Nicolas Perkowski<sup>3</sup>

<sup>1</sup>Lawrence Berkeley National Laboratory, Berkeley, California, 94720, USA

<sup>2</sup>University of Oxford, Mathematical Institute, Oxford, UK and

Freie Universität Berlin, Arnimallee 6, 14195 Berlin, Germany

<sup>3</sup>Freie Universität Berlin, Arnimallee 7, 14195 Berlin, Germany,  
and Max-Planck Institute for Mathematics in the Sciences, Leipzig, Germany

January 13, 2026

## Abstract

We consider stochastic particle dynamics on hypersurfaces represented in Monge gauge parametrization. Starting from the underlying Langevin system, we derive the surface Dean–Kawasaki (DK) equation and formulate it in the martingale sense. The resulting SPDE explicitly reflects the geometry of the hypersurface through the induced metric and its differential operators. Our framework accommodates both pairwise interactions and environmental potentials, and we extend the analysis to evolving hypersurfaces driven by an SDE that interacts with the particles, yielding the corresponding surface DK equation for the coupled surface–particle system. We establish a weak uniqueness result in the non-interacting case, and we develop a finite-volume discretization preserving the fluctuation–dissipation relation. Numerical experiments illustrate equilibrium properties and dynamical behavior influenced by surface geometry and external potentials.

**Keywords:** Dean–Kawasaki equation, interacting particle systems, fluctuating membrane, surface SPDEs, FVM

**MSCMSC Classification:** 60H15, 60J60, 60H35, 65C30, 60K35

## 1 Introduction

Transport processes constrained to curved surfaces arise in a wide range of physical, biological, and chemical systems. Whenever the motion of microscopic particles: proteins, agents, etc. – is restricted to a lower-dimensional manifold, the interplay between geometry, stochasticity, and interactions becomes an important feature of the resulting dynamics. Such scenarios appear for example in statistical physics (active or passive particles constrained to manifolds), agent based modeling in social dynamics (target tracking system on the planet [3]), molecular dynamics [4, 23, 25], or consensus-based optimization [16].

Cell biology, in particular, offers a representative setting for such systems [1, 26]. The cell membrane is a (thermally fluctuating) surface composed of lipids and embedded proteins, and it hosts numerous processes crucial for cellular function. A prototypical membrane model is the thermally excited Helfrich elastic membrane [27, 28]. Lateral diffusion of membrane-bound molecules is one of the primary mechanisms governing signaling, transport, and regulation

at the cellular interface (see, e.g., [1]). The study of such processes has attracted sustained attention over the past decades [2, 26, 31]. While some works investigate particle diffusion on static membranes [28], others concentrate on membranes with thermal fluctuations that lead to the change of the shape of a membrane over time [17, 29, 30]. Besides the interaction between particles, there is also induced interaction between the particles and the shape of the membrane.

From a mathematical perspective, these systems provide prototypical examples where geometry and noise couple in a nontrivial way, requiring new analytical and numerical tools. The particles are often modeled as interacting Brownian diffusions on manifolds. Brownian motion on a hypersurface can be defined using the Laplace–Beltrami generator [19], but can be also represented via Langevin equations. As highlighted in [27], an important advantage of the Langevin description is its flexibility to incorporate extensions that account for both particle–particle and membrane–particle interactions (for instance, active protein inclusions [24]).

We consider the case when the surface is described in the Monge gauge, meaning that it is represented as the graph of a given height function, as for example in [12]. The advantage of this representation is that all differential operators can be easily represented explicitly in global coordinate space using appropriate Euclidean differential operators.

The simulations of such particle–membrane systems are often very costly when the system becomes large, which is typically the case in the applications mentioned above. The main goal of this work is to propose a reduced model for particle systems on (evolving) curved domains with pairwise interactions and particle–membrane coupling, while still capturing finite-size effects. A well-established framework for such reductions is the description of the dynamics of the empirical measure through Dean–Kawasaki equation [8, 20]. The study of these equations, from both computational [11, 18] and analytical [5, 6, 10, 9, 14, 15, 21, 22] perspectives, has evolved rapidly over the last decade. Nevertheless, to the best of our knowledge, no counterpart of the Dean–Kawasaki equation has been derived for particle systems on curved, evolving domains. Closing this gap is the main contribution of the present work.

Starting from the Langevin dynamics describing both pairwise particle interactions and particle–membrane coupling, we apply Itô’s formula to derive the evolution equation for the empirical distribution. As in the flat case, a key difficulty in this derivation is that the resulting noise term is not closed, making a direct formulation in terms of the empirical density problematic. For this reason, a more appropriate viewpoint is provided by the martingale formulation, which allows us to characterize the quadratic variation of the noise. The martingale formulation suggests a formal nonlinear transport-type equation for the (formal) density of the empirical distribution, which serves as basis for numerical discretizations. A distinct feature arising on hypersurfaces concerns the choice of the correct noise representation: in this geometric setting, one may consider the (formal) density of the empirical distribution either with respect to Lebesgue measure on the coordinate space or with respect to the intrinsic surface area measure. We analyze both possibilities, which lead to two different formulations of the resulting equation. To justify the chosen noise structure, we further establish that the fluctuation–dissipation relation is satisfied. In addition, we prove weak uniqueness for the surface Dean–Kawasaki equation.

For the numerical approximation, we exploit the conservative structure of the equation and employ a finite-volume discretization in space combined with an Euler–Maruyama scheme in time. A major challenge arises from the fact that the matrices appearing in the divergence formulation are generally full, leading to coupling through off-diagonal terms. To address this

issue, we adopt one-sided approximations of the surface gradient operators and construct a discrete metric divergence operator that is adjoint to the discrete gradient with respect to the surface area measure. We show that with this type of the discretization, the fluctuation dissipation relation is preserved. We present two main classes of numerical experiments. The first focuses on equilibrium statistics of the linearized surface Dean–Kawasaki equation, while the second examines how the interplay between particle dynamics and geometry influences the spreading of particles. The results indicate that the surface geometry plays a central role in governing how particles move and how they ultimately spread across the domain. Additional numerical experiments illustrate how an external potential impacts the particle dynamics.

The paper is organized as follows. Section 2 reviews the geometric preliminaries, introducing the Monge gauge parametrization and the differential operators required for the formulation of the surface equation. Section 3 presents the derivation of the surface Dean–Kawasaki equation starting from the underlying Langevin dynamics. To highlight the main ideas, we first examine the case of independent Brownian particles on a hypersurface and then derive the full surface Dean–Kawasaki equation for interacting particles coupled to an evolving hypersurface whose motion is governed by a stochastic differential equation. In Section 4, we present a finite volume discretization of the two-dimensional surface Dean–Kawasaki equation, including the effect of a possible external potential. Section 5 provides computational examples that validate the proposed numerical scheme in the absence of an external potential and demonstrate its performance when an external potential is present.

## 2 Preliminaries

### 2.1 Geometric setting

We will consider surface that can be presented in Monge gauge (graph) parametrization. Let<sup>1</sup>  $D = \prod_{i=1}^d (\mathbb{R}/L_i \mathbb{Z})$ , for  $L_1, \dots, L_d > 0$ . For a  $C^3$  height (Monge gauge) function  $H : D \rightarrow \mathbb{R}$ , the surface  $\Gamma$  is then parametrized over  $D$  in the following way

$$\Gamma = \{(x, H(x)) : x \in D\}.$$

Hence,  $\Gamma$  is the graph of a function  $H$  and is parametrized by the Monge gauge map  $\Phi : D \rightarrow \mathbb{R}^{d+1}$  with  $\Phi(x) := (x, H(x))$ ,  $x \in D$ , and the tangent basis vectors are given by

$$\tau_i = \partial_i \Phi = e_i + (\partial_i H) e_{d+1}, \quad i = 1, \dots, d,$$

where  $e_i$  denotes the  $i$ -th canonical basis vector of  $\mathbb{R}^d$ . Then the induced metric is given by

$$G(x) = [\tau_i \cdot \tau_j]_{i,j=1}^d = D\Phi(x)^T D\Phi(x) = I_d + \nabla H(x) \otimes \nabla H(x) \in \mathbb{R}^{d \times d}, \quad x \in D \subset \mathbb{R}^d,$$

where  $D\Phi$  denotes the Jacobian matrix of the parametrization  $\Phi$  and we denote the determinant of the matrix  $G$  by

$$|G|(x) := \det(G(x)) = 1 + |\nabla H(x)|^2.$$

It follows directly that for a unit vector  $e \in \mathbb{R}^d$

$$1 \leq e \cdot G(x)e \leq |G|(x) \quad \forall x \in D,$$

---

<sup>1</sup>The analysis would extend without difficulty to  $D = \mathbb{R}^d$  under suitable assumptions on  $H$ , or to domains  $D \subset \mathbb{R}^d$  with (piecewise) smooth boundary under homogeneous Neumann boundary conditions.

hence  $G$  is uniformly elliptic and  $C^2$ . The inverse matrix  $G^{-1}$  has components that we denote by  $G^{ij}$  and is given by

$$G^{-1} = \mathbf{I}_d - \frac{\nabla H \otimes \nabla H}{1 + |\nabla H|^2},$$

where  $\mathbf{I}_d$  is the identity matrix in  $\mathbb{R}^{d \times d}$ . The unit outward normal is given by

$$n = \frac{1}{\sqrt{|G|}} \begin{pmatrix} -\nabla H \\ 1 \end{pmatrix}.$$

The surface area element is defined as

$$\nu(dx) := \sqrt{|G|(x)} dx \quad (1)$$

and for a scalar field  $\tilde{f} : \Gamma \rightarrow \mathbb{R}$ , after using the change of the coordinates  $y = \Phi(x)$ , the surface measure  $S$  on  $\Gamma$  is given by

$$\int_{\Gamma} \tilde{f}(y) dS(y) = \int_D \tilde{f}(\Phi(x)) \sqrt{|G|(x)} dx. \quad (2)$$

Next, we introduce differential operators. To define the tangential gradient, we introduce the projection onto the tangent space, denoted by  $\Pi : \mathbb{R}^{d+1} \rightarrow \mathbb{R}^d$ , which is defined as

$$\Pi := \mathbf{I}_{d+1} - n \otimes n.$$

For the smooth function  $\tilde{f} : \Gamma \rightarrow \mathbb{R}$  defined on the surface, the tangential gradient is defined as

$$\nabla_{\Gamma} \tilde{f}(y) := \Pi(y) \nabla \tilde{f}(y), \quad y \in \Gamma, \quad (3)$$

where the ambient gradient is applied to any extension of the function  $\tilde{f}$  to the neighborhood of the surface, but since it can be shown that the value does not depend on this extension we use the same notation  $\tilde{f}$ . In the Monge gauge representation of  $\Gamma$ , every function  $\tilde{f} : \Gamma \rightarrow \mathbb{R}$  on the surface can be identified with a function on the coordinate domain  $D$ :

$$f : D \rightarrow \mathbb{R}, \quad f(x) := \tilde{f}(\Phi(x)).$$

Using the chain rule, we can express the tangent vector  $\nabla_{\Gamma}$  in local coordinates in the following way:

$$\nabla_{\Gamma} \tilde{f}(\Phi(x)) = D\Phi(x)G^{-1}(x)\nabla f(x) = \begin{pmatrix} G^{-1}\nabla f(x) \\ \nabla H(x) \cdot G^{-1}(x)\nabla f(x) \end{pmatrix}, \quad x \in D.$$

Since we will consider everything in the coordinate domain, we define the metric gradient of the function  $f : D \rightarrow \mathbb{R}$  as the  $d$ -dimensional upper block of the tangential gradient:

$$\nabla_G f := G^{-1}\nabla f. \quad (4)$$

Furthermore, we define the metric divergence, that is the adjoint of the metric gradient, in the following way

$$\int_D (\operatorname{div}_G \cdot w) \varphi \sqrt{|G|} dx := - \int_D (w, \nabla_G \varphi)_G \sqrt{|G|} dx := - \int_D w \cdot G \nabla_G \varphi \sqrt{|G|} dx, \quad \varphi \in C_c^{\infty}(D),$$

where

$$(a, b)_G := a \cdot Gb.$$

Using the definition of the surface gradient and chain rule, the metric divergence can be written using the standard Euclidean divergence as

$$\operatorname{div}_G f = \frac{1}{\sqrt{|G|}} \nabla \cdot (\sqrt{|G|} f). \quad (5)$$

We define the Laplace-Beltrami operator in the natural way

$$\Delta_G := \operatorname{div}_G \nabla_G = \frac{1}{\sqrt{|G|}} \nabla \cdot (\sqrt{|G|} G^{-1} \nabla). \quad (6)$$

Note that  $\Delta_G$  is symmetric in  $L^2(\nu)$ .

## 2.2 Brownian motion on the hypersurface

We recall the definition of a Brownian motion on a hypersurface [12], which is a special case of a more general definition given in [19, Proposition 3.2.1].

For convenience, from now on we periodically extend functions on  $D$  to  $\mathbb{R}^d$ . For example, this allows us to directly describe the Brownian motion on the hypersurface by an SDE, instead of having to consider solutions modulo  $\prod_{i=1}^d L_i \mathbb{Z}$ .

**Definition 1.** Let  $(\Omega, \mathcal{F}, \mathbb{P})$  be a complete probability space endowed with a right-continuous filtration  $(\mathcal{F}_t)_{t \geq 0}$ . An  $\mathbb{R}^d$ -valued process  $X$  defined on  $\Omega \times [0, T]$  is called a Brownian motion on  $\Gamma$  started at  $X_0 = x \in \mathbb{R}^d$  if  $X$  is adapted, almost surely continuous, and if for every  $f \in C^2(\mathbb{R}^d)$ ,

$$f(X_t) - f(x) - \int_0^t \Delta_G f(X_s) ds, \quad t \geq 0,$$

is a local martingale starting from 0, where  $\Delta_G$  is the Laplace-Beltrami operator in local coordinates on  $\mathbb{R}^d$ , given by (6).

The process  $X$  has the following representation through an SDE:

$$dX_t = \underbrace{\frac{1}{\sqrt{|G|}} \nabla \cdot (\sqrt{|G|} G^{-1})}_{=: b}(X_t) dt + \sqrt{2} G^{-1/2}(X_t) dB_t, \quad (7)$$

where  $B$  is a  $d$ -dimensional standard Brownian motion. Note that the coefficients of the SDE are Lipschitz continuous, because  $H \in C^3$  is periodic and thus its derivatives are bounded. For  $H \in C^2$  we would get a singularity in the drift coefficient, and it is well understood that the noise would regularize this singularity [32]; for simplicity we stick with the Lipschitz setting.

**Remark 2.** Note that there is another way of defining the Brownian motion on  $\Gamma$  using the projection on the tangent space and the ambient Brownian motion  $B^{d+1}$  from  $\mathbb{R}^{d+1}$  [13, Example 8.4]. More precisely, the process defined as  $dY_t := \Pi \circ dB_t^{d+1}$ , where  $\circ$  denotes the Stratonovich integral, and whose infinitesimal generator is given by the Laplace-Beltrami operator.

### 3 Derivation of surface Dean–Kawasaki equation

#### 3.1 Surface Dean–Kawasaki equation on a fixed surface: non-interacting, potential-free case

Let now  $X^1, \dots, X^N$  be i.i.d. copies of the Brownian motion  $X$  given by (7), potentially with different initial conditions. Furthermore, let

$$\mu_t = \frac{1}{N} \sum_{i=1}^N \delta_{X_t^i} \quad (8)$$

be the empirical distribution at time  $t$ . Then Itô’s formula shows that for  $f \in C_b(D)$  the following process is a continuous martingale:

$$M_t^f = \mu_t(f) - \mu_0(f) - \int_0^t \mu_s(\Delta_G f) ds, \quad (9)$$

with quadratic variation

$$d\langle M^f \rangle_t = \frac{2}{N^2} \sum_{i=1}^N |G^{-1/2} \nabla f(X_t^i)|^2 dt = \frac{2}{N} \mu_t(|G^{-1/2} \nabla f(X_t^i)|^2) dt. \quad (10)$$

While the martingale problem for  $\mu$  has a unique solution [22], the analysis of numerical approximation schemes naturally leads us to consider the associated nonlinear Dean–Kawasaki equation, which (formally) provides a continuum description of the particle system.

Indeed, let us pretend that  $\mu_t$  has a density with respect to Lebesgue measure, which we denote by  $\rho_t^\lambda$ . Then

$$\mu_s(f) = \langle \rho_s^\lambda, f \rangle_{L^2(D)} \quad (11)$$

and

$$\mu_s(\Delta_G f) = \langle \rho_s^\lambda, \Delta_G f \rangle_{L^2(D)} = \langle \Delta_G^* \rho_s^\lambda, f \rangle_{L^2(D)}, \quad (12)$$

where the adjoint is computed with respect to Lebesgue measure,

$$\Delta_G^* f = -\nabla \cdot (bf) + \sqrt{2} D^2 : (G^{-1} f),$$

with  $A : B = \text{Tr}(AB)$ . To find a formal representation of the martingale as a stochastic integral, let  $W$  be a cylindrical Wiener process with identity covariance on the Hilbert space  $U = L^2(D; \mathbb{R}^d)$  with inner product  $\langle f, g \rangle_U = \int_D f(x) \cdot g(x) dx$ , i.e. formally (because  $W(t)$  does not actually take values in  $U$ ) it holds  $\mathbb{E}[\langle W(t), f \rangle_U^2] = t \|f\|_U^2$ . Then

$$\begin{aligned} \int_0^t \mu_s(|G^{-1/2} \nabla f(X_t^i)|^2) ds &= \int_{[0,t] \times D} \rho_s^\lambda(x) |G^{-1/2}(x) \nabla f(x)|^2 ds dx, \\ &= \int_0^t \left\| \sqrt{\rho_s^\lambda} G^{-1/2} \nabla f \right\|_U^2 ds \\ &= \left\langle \int_0^t \langle \sqrt{\rho_s^\lambda} G^{-1/2} \nabla f, dW_s \rangle_U \right\rangle_t \\ &= \left\langle \int_0^t \left\langle f, \nabla \cdot (\sqrt{\rho_s^\lambda} G^{-1/2} dW_s) \right\rangle_{L^2(D)} \right\rangle_t, \end{aligned} \quad (13)$$

where we used that  $-\nabla \cdot$  is the adjoint of  $\nabla$ , as an operator from  $U$  to  $L^2(D)$ . Combining (9), (10), (11), (12) and (13), we obtain the Dean–Kawasaki equation for the density  $\rho^\lambda$ :

$$d\rho_t^\lambda = \Delta_G^* \rho_t^\lambda dt + \sqrt{\frac{2}{N}} \nabla \cdot \left( \sqrt{\rho_t^\lambda} G^{-1/2} dW_t \right). \quad (14)$$

### 3.1.1 Intrinsic representation

We next consider the formulation with respect to the surface area measure  $\nu$  given by (1). This choice is natural, as it incorporates the geometric structure of the surface. We denote by  $\rho^\nu$  the formal density of  $\mu$  with respect to  $\nu$ . Then for

$$H := L^2(D, \nu), \quad (15)$$

we have

$$\mu_s(f) = \langle \rho_s^\nu, f \rangle_H \quad (16)$$

and

$$\mu_s(\Delta_G f) = \langle \rho_s^\nu, \Delta_G f \rangle_H = \langle \Delta_G \rho_s^\nu, f \rangle_H, \quad (17)$$

where we used that  $\Delta_G$  is self-adjoint in  $H$ . To find a formal representation of the martingale as a stochastic integral, let  $W^G$  be a cylindrical Wiener process on the Hilbert space

$$U = L^2(D, \nu; \mathbb{R}^d, (\cdot, \cdot)_G), \quad \langle f, g \rangle_U = \int_D (f(x), g(x))_{G(x)} \sqrt{|G(x)|} dx, \quad (18)$$

with identity covariance, i.e. formally (because  $W_t^G$  does not take values in  $U$ )

$$\mathbb{E}[\langle W_t^G, f \rangle_U^2] = t \|f\|_U^2. \quad (19)$$

Then, noting that  $|G^{-1/2} \nabla f|^2 = \|\nabla_G f\|_G^2$ ,

$$\begin{aligned} \int_0^t \mu_s(|G^{-1/2} \nabla f(X_t^i)|^2) ds &= \int_0^t \|\sqrt{\rho_s^\nu} \nabla_G f\|_U^2 ds \\ &= \left\langle \int_0^t \langle \sqrt{\rho_s^\nu} \nabla_G f, dW_s^G \rangle_U \right\rangle_t \\ &= \left\langle \int_0^t \langle f, \text{div}_G(\sqrt{\rho_s^\nu} dW_s^G) \rangle_{L^2(D)} \right\rangle_t, \end{aligned} \quad (20)$$

where we used that  $-\text{div}_G$  is the adjoint of  $\nabla_G$ , as an operator from  $U$  to  $L^2(D)$ . Combining (9), (10), (16), (17) and (20), we obtain the surface Dean–Kawasaki equation for the density  $\rho^\nu$ :

$$d\rho_t^\nu = \Delta_G \rho_t^\nu dt + \sqrt{\frac{2}{N}} \text{div}_G \left( \sqrt{\rho_t^\nu} dW_t^G \right). \quad (21)$$

**Remark 3** (On the interpretation of  $W^G$ ). Note that statistically  $W^G = |G|^{-1/4} G^{-1/2} W$ , where  $W$  is a standard  $\mathbb{R}^d$ -valued space-time noise. Indeed, for  $f \in U$  it holds

$$\mathbb{E} \left[ \left\langle |G|^{-1/4} G^{-1/2} W_t, f \right\rangle_U^2 \right] = \mathbb{E} \left[ \left\langle W_t, |G|^{1/4} G^{1/2} f \right\rangle_{L^2(D, \mathbb{R}^d)}^2 \right] = t \| |G|^{1/4} G^{1/2} f \|_{L^2(D, \mathbb{R}^d)}^2 = t \|f\|_U^2,$$

which coincides with (19).

Starting from the intrinsic formulation of the surface Dean–Kawasaki Equation (21), together with the representation of the noise and the definitions of the metric differential operators (4) and (5), we obtain a coordinate representation of the equation in terms of local coordinates and standard Euclidean differential operators:

$$d\rho_t^\nu = \frac{1}{\sqrt{|G|}} \nabla \cdot (\sqrt{|G|} G^{-1} \nabla \rho_t^\nu) dt + \sqrt{\frac{2}{N}} \frac{1}{\sqrt{|G|}} \nabla \cdot (\sqrt{\rho_t^\nu} |G|^{1/4} G^{-1/2} dW_t), \quad (22)$$

where  $W$  is the usual  $\mathbb{R}^d$ -valued space-time white noise. This formulation will serve as the basis for the numerical discretization.

**Remark 4.** *If we start from the Brownian particles that are given via Stratonovich formulation on  $\Gamma$ , as described in Remark 2, the martingale formulation of the Dean–Kawasaki equation for the corresponding empirical distribution  $\mu^\Gamma$  is*

$$d\mu_t^\Gamma(f) = \mu_t^\Gamma(\Delta_\Gamma f) dt + dM_t^f,$$

where  $\Delta_\Gamma = \operatorname{div}_\Gamma \nabla_\Gamma$ , with  $\nabla_\Gamma$  as in (3), with  $-\operatorname{div}_\Gamma$  the adjoint of  $\nabla_\Gamma$  as an operator from  $L^2(\Gamma, S)$  to  $L^2(\Gamma, S; T\Gamma)$  (recall that the surface measure  $S$  is defined in (2)), and where  $M^f$  is a continuous martingale with quadratic variation

$$d\langle M^f \rangle_t = \frac{2}{N} \mu_t^\Gamma(|\nabla_\Gamma f|^2) dt.$$

Next, if we pretend that  $\mu^\Gamma$  has a density  $\rho^S$  with respect to the surface measure  $S$  defined in (2), then for

$$H := L^2(\Gamma, S) \quad \text{and} \quad U := L^2(\Gamma, S; T\Gamma),$$

and for  $W^S$  a cylindrical Wiener process with identity covariance on  $U$ ,

$$\mathbb{E}[\langle W_t^S, f \rangle_U^2] = t \|f\|_U^2,$$

we have

$$\mu_t^\Gamma(|\nabla_\Gamma f|^2) dt = \|\sqrt{\rho_t^S} \nabla_\Gamma f\|_U^2 dt = d\langle \int_0^\cdot \langle \sqrt{\rho_s^S} \nabla_\Gamma f, dW_s^S \rangle_U \rangle_t = \langle \int_0^\cdot \langle f, \operatorname{div}_\Gamma \left( \sqrt{\rho_s^S} dW_s^S \right) \rangle_H \rangle_t.$$

Hence, using also that  $\Delta_\Gamma$  is self-adjoint in  $L^2(\Gamma, S)$ , the surface Dean–Kawasaki equation for  $\rho^S$  is

$$d\rho_t^S = \Delta_\Gamma \rho_t^S dt + \sqrt{\frac{2}{N}} \operatorname{div}_\Gamma \left( \sqrt{\rho_t^S} dW_t^S \right).$$

### 3.1.2 Fluctuation dissipation relation

The linearization of the intrinsic surface Dean–Kawasaki Equation (21) around its time-stationary mean field limit

$$\bar{\rho}^\nu \equiv \frac{1}{\nu(D)}$$

is given by the Ornstein–Uhlenbeck process

$$dZ_t = \Delta_G Z_t dt + \sqrt{\frac{2}{N}} \operatorname{div}_G \left( \sqrt{\bar{\rho}^\nu} dW_t^G \right). \quad (23)$$

Then for the spaces  $H$  and  $U$  defined by (15) and (18) respectively, the operator  $A := \Delta_G$  is a self-adjoint operator on  $H$ , the cylindrical Wiener process  $W^G$  on  $U$  has covariance  $Q := \text{Id}$ , and  $B := \sqrt{\frac{2}{N}\bar{\rho}^\nu} \text{div}_G$  is a linear operator from  $U$  to  $H$  with adjoint  $B^* = -\sqrt{\frac{2}{N}\bar{\rho}^\nu} \nabla_G$ . By [7], Section 11.3, the covariance  $C$  of the centered Gaussian equilibrium distribution satisfies

$$AC + CA = -BQB^*,$$

which implies that

$$C = \frac{\bar{\rho}^\nu}{N} \text{Id},$$

which matches the statistics of the coarse-grained particle system and confirms the choice of the fluctuating noise in (21). Hence, the fluctuation dissipation relation is fulfilled.

Furthermore, the formal covariance function of  $Z$  at stationarity is given by

$$\mathbb{E}[Z(x)Z(y)] = \frac{\bar{\rho}^\nu}{N\sqrt{|G|(x)}}\delta(x-y), \quad (24)$$

which we want to preserve under numerical discretization.

### 3.2 Surface Dean–Kawasaki equation for interacting particle system on fixed hypersurface

We introduce potentials that lead to invariant Gibbs measures: Let  $V \in C_b^2(D; \mathbb{R})$  and let  $U \in C_b^2(D \times D; \mathbb{R})$  be symmetric and consider the following (non-normalized) measure on  $D^N$

$$\nu_N(dx) := \exp\left(-\sum_i V(x_i) - \frac{1}{2N} \sum_{i,j} U(x_i, x_j)\right) \prod_{i=1}^N \sqrt{|G|(x_i)} dx_i.$$

Our goal is to find a reversible diffusion process  $(X^1, \dots, X^N)$  with invariant measure  $\nu_N$ , in analogy with the usual Langevin diffusion. This will be based on the following computation.

**Remark 5.** *The operator  $\text{div}_G$  satisfies the following Leibniz type rule:*

$$\text{div}_G(fg) = \frac{1}{\sqrt{|G|}} \nabla \cdot (\sqrt{|G|} fg) = \frac{1}{\sqrt{|G|}} \nabla \cdot (\sqrt{|G|} f) g + \frac{1}{\sqrt{|G|}} \sqrt{|G|} f \nabla \cdot g = (\text{div}_G f)g + f \cdot \nabla g.$$

For arbitrary  $F \in C^2(D^N)$ , the operator

$$\mathcal{L}_{N,F} = e^F \sum_{i=1}^N \text{div}_{G,x_i}(e^{-F} \nabla_{G,x_i}),$$

is symmetric with respect to the measure  $e^{-F(x)} \prod_{i=1}^N \sqrt{|G|(x_i)} dx_i$ . Using the Leibniz rule from Remark 5, the operator  $\text{div}_G$  can be rewritten as follows:

$$\mathcal{L}_{N,F} = \sum_{i=1}^N (\Delta_{G,x_i} - \nabla_{x_i} F \cdot \nabla_{G,x_i}) = \sum_{i=1}^N (\Delta_{G,x_i} - \nabla_{G,x_i} F \cdot \nabla_{x_i}).$$

Choosing  $F(x) = \sum_k V(x_k) + \frac{1}{2N} \sum_{k,\ell} U(x_k, x_\ell)$ , we obtain

$$\nabla_{x_i} F(x) = \nabla V(x_i) + \frac{1}{2N} \sum_\ell \nabla_{x_i} U(x_i, x_\ell) + \frac{1}{2N} \sum_k \nabla_{x_i} U(x_k, x_i) = \nabla V(x_i) + \frac{1}{N} \sum_j \nabla_{x_i} U(x_i, x_j),$$

where we used that  $U$  is symmetric.

This leads to the definition of a Langevin diffusion for  $\nu_N$ :

**Definition 6.** *We call a stochastic process  $(X^1, \dots, X^N)$  with values in  $D^N$  the Langevin diffusion with invariant measure  $\nu_N$ , if it is a Markov process with generator*

$$\begin{aligned} \mathcal{L}_N &= \sum_{i=1}^N \left( - \left( \nabla_G V(x_i) + \frac{1}{N} \sum_{j=1}^N \nabla_{G,x_i} U(x_i, x_j) \right) \cdot \nabla_{x_i} + \Delta_{G,x_i} \right) \\ &= \sum_{i=1}^N \left( - \left( \nabla_G V(x_i) + \frac{1}{N} \sum_{j=1}^N \nabla_{G,x_i} U(x_i, x_j), \nabla_{G,x_i} \right)_G + \Delta_{G,x_i} \right). \end{aligned}$$

The SDE for this generator is

$$\begin{aligned} dX_t^i &= b(X_t^i)dt - \nabla_G V(X_t^i)dt - \frac{1}{N} \sum_{j=1}^N \nabla_{G,x_i} U(X_t^i, X_t^j)dt + \sqrt{2}G^{-1/2}(X_t^i)dB_t^i \quad (25) \\ &= b(X_t^i)dt - \nabla_G V(X_t^i)dt - \int_D \nabla_{G,x_i} U(X_t^i, x) \mu_t(dx)dt + \sqrt{2}G^{-1/2}(X_t^i)dB_t^i, \end{aligned}$$

where  $b$  is defined by (7). Let  $\mu$  be the empirical distribution. In a similar way as for (14), we derive the Dean–Kawasaki equation for the formal density  $\rho^\lambda$  of  $\mu$  with respect to Lebesgue measure:

$$d\rho_t^\lambda = \Delta_G^* \rho_t^\lambda dt + \nabla \cdot \left( \left( \nabla_G V + \int_D \nabla_G U(\cdot, x) \rho_t^\lambda(x) dx \right) \rho_t^\lambda \right) dt + \sqrt{\frac{2}{N}} \nabla \cdot \left( \sqrt{\rho_t^\lambda} G^{-1/2} dW \right).$$

The surface Dean–Kawasaki equation in the intrinsic form for the (formal) density  $\rho^\nu$  with respect to the surface area element  $\nu$  is

$$d\rho_t^\nu = \Delta_G \rho_t^\nu dt + \operatorname{div}_G \left( \left( \nabla_G V + \int_D \nabla_G U(\cdot, x) \rho_t^\nu(x) dx \right) \rho_t^\nu \right) dt + \sqrt{\frac{2}{N}} \operatorname{div}_G (\sqrt{\rho^\nu} dW^G). \quad (26)$$

### 3.3 The surface Dean–Kawasaki equation on a moving, interacting surface.

We now consider a more general setting in which the hypersurface is moving and the induced metric  $G$  is governed by a stochastic process  $\eta$  and is therefore time-dependent. Furthermore, we allow the particles and the hypersurface to interact. A typical example of a moving surface is given by the ultraviolet-truncated Langevin dynamics of a Helfrich elastic membrane, which can be represented as a multidimensional Ornstein–Uhlenbeck process; see [12, Section 4] for further details.

More precisely, we assume that  $\eta$  solves another stochastic differential equation, coupled with the empirical measure of the particle system, and that  $G_t = G(\cdot, \eta_t)$ :

$$d\eta_t = a(\eta_t, \mu_t)dt + \sigma(\eta_t, \mu_t)dB_t. \quad (27)$$

Moreover, we assume that

$$dX_t^i = b_t(X_t^i)dt - \nabla_{G_t}V(X_t^i)dt - \int_D \nabla_{G_t}U(X_t^i, x)\mu_t(dx)dt + \sqrt{2}G_t^{-1/2}(X_t^i)dB_t^i,$$

where  $B$  is independent from  $(B^1, \dots, B^N)$ , and

$$b_t(x) = \frac{1}{\sqrt{|G_t|(x)}} \nabla_x \cdot \left( \sqrt{|G_t|(x)} G_t^{-1}(x) \right).$$

Then, the Dean–Kawasaki equation for the formal density  $\rho^\lambda$  of the empirical distribution with respect to Lebesgue measure is given by

$$\begin{aligned} d\rho_t^\lambda &= \Delta_{G_t}^* \rho_t^\lambda dt + \nabla \cdot \left( \left( \nabla_{G_t}V + \int \nabla_{G_t}U(\cdot, x)\rho_t^\lambda(x)dx \right) \rho^\lambda \right) dt \\ &\quad + \sqrt{\frac{2}{N}} \nabla \cdot \left( \sqrt{\rho^\lambda} G_t^{-1/2} dW_t \right), \\ d\eta_t &= a(\eta_t, \rho_t^\lambda)dt + \sigma(\eta_t, \rho_t^\lambda)dB_t, \end{aligned}$$

where the space-time white noise  $W$  is independent of  $B$ .

Next, we derive the equation for the formal density  $\rho^{\nu_t}$  with respect to

$$\nu_t(dx) := g_t(x)dx := \sqrt{|G_t(x)|}dx.$$

Since formally  $\rho^{\nu_t}\nu_t = \mu_t$ , from Itô's formula we have

$$d\rho^{\nu_t}\nu_t(f) = \rho^{\nu_t}\nu_t \left( \Delta_{G_t}f - \left( \nabla_{G_t}V + \int_D \nabla_{G_t}U(\cdot, x)\rho_t^{\nu_t}\nu_t(dx), \nabla_{G_t}f \right)_{G_t} \right) dt + dM_t^f, \quad (28)$$

with a continuous martingale  $M^f$  that satisfies

$$d\langle M_t^f \rangle = \frac{2}{N} \rho_t^{\nu_t}\nu_t(|\nabla_{G_t}f|_{G_t}^2)dt, \quad d\langle M^f, B^\eta \rangle_t = 0.$$

Thus, we can represent the martingale as follows: Let  $W$  be a space-time white noise in  $L^2(D; \mathbb{R}^d)$ , independent of  $B^\eta$ , and let

$$W_t^G := \int_0^t g_s^{-1/2} G_s^{-1/2} dW_s. \quad (29)$$

Let also

$$U_t := L^2(D, \nu_t; \mathbb{R}^d, (\cdot, \cdot)_{G_t}),$$

so that formally for any adapted process  $u$  with  $\int_0^T \|u_t\|_{U_t}^2 dt < \infty$  for all  $T > 0$ :

$$d\left\langle \int_0^\cdot \langle u_s, dW_s^G \rangle_{U_s} \right\rangle_t = d\left\langle \int_0^\cdot \langle g_t^{1/2} G_t^{1/2} u_s, dW_s \rangle_{L^2(D; \mathbb{R}^d)} \right\rangle_t = \|g_t^{1/2} G_t^{1/2} u_t\|_{L^2(D; \mathbb{R}^d)}^2 dt = \|u_t\|_{U_t}^2 dt.$$

Then we have with  $H_t := L^2(D, \nu_t)$

$$\begin{aligned} \frac{N}{2} d\langle M_t^f \rangle &= \rho_t^{\nu_t}\nu_t(|\nabla_{G_t}f|_{G_t}^2)dt = \left\| \sqrt{\rho_t^{\nu_t}} \nabla_{G_t}f \right\|_{U_t}^2 dt = d\left\langle \int_0^\cdot \left\langle \sqrt{\rho_t^{\nu_t}} \nabla_{G_s}f, dW_s^G \right\rangle_{U_s} \right\rangle_t \\ &= d\left\langle \int_0^\cdot \left\langle f, \operatorname{div}_{G_s} \left( \sqrt{\rho_s^{\nu_s}} dW_s^G \right) \right\rangle_{H_s} \right\rangle_t. \end{aligned}$$

Now we integrate  $\Delta_{G_t}$  and  $\nabla_{G_t}$  in (28) by parts to obtain the equation

$$\begin{aligned} d\langle \rho_t^{\nu_t}, f \rangle_{H_t} &= \left\langle \Delta_{G_t} \rho_t^{\nu_t} + \operatorname{div}_{G_t} \left( \left( \nabla_{G_t} V + \int \nabla_{G_t} U(\cdot, x) \rho_t^{\nu_t}(x) \nu_t(dx) \right) \rho_t^{\nu_t} \right), f \right\rangle_{H_t} dt \\ &\quad + \sqrt{\frac{2}{N}} \langle f, \operatorname{div}_{G_t} (\sqrt{\rho^{\nu_t}} dW_t^G) \rangle_{H_t}, \end{aligned}$$

which we can rewrite as

$$\begin{aligned} d(\rho_t^{\nu_t} g_t) &= \left( \Delta_{G_t} \rho_t^{\nu_t} + \operatorname{div}_{G_t} \left( \left( \nabla_{G_t} V + \int \nabla_{G_t} U(\cdot, x) \rho_t^{\nu_t}(x) \nu_t(dx) \right) \rho_t^{\nu_t} \right) \right) g_t dt \\ &\quad + \sqrt{\frac{2}{N}} g_t \operatorname{div}_{G_t} (\sqrt{\rho^{\nu_t}} dW_t^G). \end{aligned}$$

Since this is not a closed equation, we divide both sides by  $g_t$ . Using that

$$dg_t^{-1} = -g_t^{-2} dg_t + g_t^{-3} d\langle g \rangle_t, \quad d\left\langle g^{-1}, \int_0^t f_s W_s^G \right\rangle_t = 0,$$

we obtain the interacting surface Dean–Kawasaki equation on a time-dependent surface with particle-surface coupling:

$$\begin{aligned} d\rho_t^\nu &= d(\rho_t^{\nu_t} g_t) g_t^{-1} \\ &= g_t^{-1} d(\rho_t^{\nu_t} g_t) + (\rho_t^{\nu_t} g_t) dg_t^{-1} + d\langle g^{-1}, \rho^\nu g \rangle_t \\ &= \left( \Delta_{G_t} \rho_t^{\nu_t} + \operatorname{div}_{G_t} \left( \left( \nabla_{G_t} V + \int \nabla_{G_t} U(\cdot, x) \rho_t^{\nu_t}(x) \nu_t(dx) \right) \rho_t^{\nu_t} \right) \right) dt \\ &\quad + \sqrt{\frac{2}{N}} \operatorname{div}_{G_t} (\sqrt{\rho^{\nu_t}} dW_t^G) - \rho_t^{\nu_t} (g_t^{-1} dg_t - g_t^{-2} d\langle g \rangle_t). \end{aligned} \tag{30}$$

The rigorous formulation of the surface Dean–Kawasaki equation is given in terms of a martingale problem, similarly to [21, 22]. In the following definition,  $\mathcal{P}(D)$  denotes the probability measures on  $D$ .

**Definition 7** (Martingale problem). *A stochastic process  $(\mu, \eta)$  in  $C(\mathbb{R}_+, \mathcal{P}(D) \times \mathbb{R}^e)$  is called a martingale solution to the sDK equation (30), if  $\eta$  is a (probabilistically) weak solution to (27) and for all  $f \in C^2(D)$  the process*

$$M_t^f = \mu_t(f) - \mu_0(f) - \int_0^t \mu_s \left( \Delta_{G_s} f - \nabla_{G_s} V \cdot \nabla f - \int \nabla_{G_s} U(\cdot, x) \mu_s(dx) \cdot \nabla f \right) ds,$$

$t \geq 0$ , is a continuous martingale with

$$\langle M^f \rangle_t = \frac{2}{N} \int_0^t \mu_s (|\nabla_{G_s} f|_{G_s}^2) ds, \quad \langle M^f, B \rangle_t = 0, \quad t \geq 0.$$

If  $U = 0$  and if  $a$  and  $\sigma$  are independent of  $\mu$ , we obtain the weak uniqueness of solutions to the martingale problem. This result is analogous to [22], although our proof is based on the well-posedness of the moment problem for  $\mu$ , rather than exact duality, and therefore it seems slightly more robust. As in [21], this could be extended to  $U \neq 0$  and to  $a$  which depends on  $\mu$ , as long as  $U$  and  $a$  can be removed by a Girsanov transform.

**Theorem 8** (Weak uniqueness). *Let  $U = 0$  and let  $a$  and  $\sigma$  be independent of  $\mu$ . Let  $\mathcal{G}_t = \mathcal{F}_t \vee \mathcal{F}_\infty^B$ ,  $t \geq 0$ , where  $\mathcal{F}_\infty^B$  is the canonical filtration generated by  $B$ . We assume that for all  $\mathcal{G}_0$ -measurable  $f \in C^2(D)$  and  $t \geq 0$  there exists a  $\mathcal{G}_0$ -measurable solution  $P_{\cdot,t}f \in C^{1,2}(\mathbb{R}_+ \times D)$  to the random Kolmogorov backward equation*

$$\partial_s P_{s,t}f = -(\Delta_{G_s} P_{s,t}f - \nabla_{G_s} V \cdot \nabla P_{s,t}f), \quad P_{t,t}f = f,$$

and that strong existence and weak uniqueness hold for (27). Then the law of the martingale solution  $(\mu, \eta)$  to the sDK Equation (30) is uniquely determined by its initial distribution.

*Proof.* We start by showing that  $\mathbb{E}[F(\mu_t) \mid \mathcal{G}_0]$  is uniquely determined by  $\text{law}(\mu_0)$  and the path  $(\eta_s)_{s \geq 0}$ , for all  $t \geq 0$  and  $F \in C(\mathcal{P}(D))$ . By a density argument and using the linearity of  $f \mapsto \mu_t(f)$ , it suffices to consider  $F(\mu) = \varphi(\mu_t(f))$  for  $f \in C^2$ , and it is convenient to allow  $\mathcal{G}_0$ -measurable random  $f \in C^2$ . Since  $\mu_t$  is a probability measure for each  $t \geq 0$ , the random variable  $\mu_t(f)$  is bounded and thus we can restrict to  $\varphi(x) = x^m$  by the Stone-Weierstraß theorem. The lemma following below this proof shows that the martingale  $M^f$  in Definition 7 remains a martingale in the filtration  $\mathcal{G}$ . We combine this with the telescope sum  $\mu_t(P_{t,t}f) - \mu_0(P_{0,t}f) = \lim_n \sum_{k=0}^{n-1} (\mu_{(k+1)t/n}(P_{(k+1)t/n,t}f) - \mu_{kt/n}(P_{kt/n,t}f))$  to show that for all  $\mathcal{G}_0$ -measurable random  $f$

$$\mu_t(P_{t,t}f) = \mu_0(P_{0,t}f) + \int_0^t \mu_s \left( (\partial_s + \Delta_{G_{\eta_s}} - \nabla_{G_{\eta_s}} V \cdot \nabla) P_{s,t}f \right) ds + M_t^{Pf} = \mu_0(P_{0,t}f) + M_t^{Pf},$$

where  $M^{Pf}$  is a continuous martingale in the filtration  $(\mathcal{G}_t)_{t \geq 0}$ , with quadratic variation

$$\langle M^{Pf} \rangle_s = \frac{2}{N} \int_0^s \mu_r (|\nabla_{G_r} P_{r,t}f|_{G_r}^2) dr.$$

In particular, we obtain from Itô's formula

$$\begin{aligned} & \mathbb{E}[(\mu_t(f)^m - \mu_0(P_{0,t}f)^m) \mid \mathcal{G}_0] \\ &= \mathbb{E} \left[ \int_0^t m \mu_s (P_{s,t}f)^{m-1} dM_s^{Pf} + \frac{m(m-1)}{N} \int_0^t \mu_s (P_{s,t}f)^{m-2} \mu_s (|\nabla_{G_s} P_{s,t}f|_{G_s}^2) ds \mid \mathcal{G}_0 \right] \\ &= \frac{m(m-1)}{N} \int_0^t \mathbb{E}[\mu_s (P_{s,t}f)^{m-2} \mu_s (|\nabla_{G_s} P_{s,t}f|_{G_s}^2) \mid \mathcal{G}_0] ds. \end{aligned} \quad (31)$$

Observe that the right hand side is  $(m-1)$ -linear in  $\mu_s$ , which allows an inductive proof of uniqueness: For  $m = 1$ , Equation (31) yields

$$\mathbb{E}[\mu_t(f) \mid \mathcal{G}_0] = \mathbb{E}[\mu_0(P_{0,t}f) \mid \mathcal{G}_0], \quad t \geq 0.$$

Assume now by induction that for all  $t \geq 0$  and all  $\mathcal{G}_0$ -measurable random  $f_1, \dots, f_{m-1} \in C^2$  the conditional expectation  $\mathbb{E}[\mu_t(f_1) \cdots \mu_t(f_{m-1}) \mid \mathcal{G}_0]$  is determined by the initial distribution of  $\mu$ . Then (31) shows that also  $\mathbb{E}[\mu_t(f)^m \mid \mathcal{G}_0]$  is uniquely determined. By polarization, also  $\mathbb{E}[\mu_t(f_1) \cdots \mu_t(f_m) \mid \mathcal{G}_0]$  is uniquely determined for all  $t \geq 0$ ,  $m \in \mathbb{N}$ , and  $\mathcal{G}_0$ -measurable random  $f_1, \dots, f_m \in C^2$ , which concludes the induction step.

By the tower property together with a monotone class argument, we then get uniqueness of  $\mathbb{E}[\Phi(\mu_t, \eta_t)]$  for all bounded and measurable  $\Phi : \mathcal{P}(E) \times \mathbb{R}^e \rightarrow \mathbb{R}$ . Now we perform another induction over the set of times  $t_1, \dots, t_n$  to show that

$$\mathbb{E}[\Phi_1(\mu_{t_1}, \eta_{t_1}) \cdots \Phi_n(\mu_{t_n}, \eta_{t_n})]$$

is uniquely determined by the initial distribution. We have just shown the case  $n = 1$ . For general  $n$ , we condition on  $\mathcal{F}_{t_{n-1}}$  and apply the previous argument to show that  $\mathbb{E}[\Phi(\mu_{t_n}, \eta_{t_n}) \mid \mathcal{F}_{t_{n-1}}]$  is uniquely determined by  $(\mu_{t_{n-1}}, \eta_{t_{n-1}})$ , i.e.

$$\mathbb{E}[\Phi_1(\mu_{t_1}, \eta_{t_1}) \cdots \Phi_{n-1}(\mu_{t_{n-1}}, \eta_{t_{n-1}}) \mathbb{E}[\Phi_n(\mu_{t_n}, \eta_{t_n}) \mid \mathcal{F}_{t_{n-1}}]] = \mathbb{E}[\Phi_1(\mu_{t_1}, \eta_{t_1}) \cdots \tilde{\Phi}_{n-1}(\mu_{t_{n-1}}, \eta_{t_{n-1}})],$$

so the claim for  $n$  follows from that for  $n - 1$ . We conclude by another monotone class argument to get the uniqueness of finite-dimensional distributions.  $\square$

In the proof we used the following presumably classical lemma, whose proof is in Appendix C.

**Lemma 9.** *Let  $(\mathcal{F}_t)_{t \geq 0}$  be a filtration and let  $M, B$  both be martingales in  $\mathcal{F}$ , such that  $B$  is a  $d$ -dimensional Brownian motion and  $\langle M, B^i \rangle \equiv 0$  for  $i \in \{1, \dots, d\}$ . Then  $M$  is a martingale in the larger filtration  $\mathcal{G}_t = \mathcal{F}_t \vee \mathcal{F}_\infty^B$ ,  $t \geq 0$ , where  $\mathcal{F}_\infty^B = \sigma(B_s : s \geq 0)$ .*

## 4 Discretization

In this section we present a finite volume discretization of the surface Dean–Kawasaki equation given by (26) in two dimensions with possible external potential, for the formal density of the empirical measure with respect to the surface area element. Note that, in order to simplify the notation, we will no longer use superscripts to indicate the reference measure, as in the previous sections, and simply write  $\rho$ .

The discretization is constructed on the domain  $D$  using the representation of the surface Dean–Kawasaki equation in local coordinates and Euclidean differential operators:

$$\begin{aligned} d\rho = \frac{1}{\sqrt{|G|}} \nabla \cdot (\sqrt{|G|} G^{-1} \nabla \rho) dt + \frac{1}{\sqrt{|G|}} \nabla \cdot (\sqrt{|G|} \rho G^{-1} \nabla V) dt \\ + \sqrt{\frac{2}{N}} \frac{1}{\sqrt{|G|}} \nabla \cdot (\sqrt{\rho} |G|^{1/4} G^{-1/2} dW). \end{aligned} \quad (32)$$

We assume that  $D$  is rectangular of dimension  $L_x \times L_y$  with periodic boundary conditions. We introduce a uniform finite volume mesh of size  $I \times J$  with mesh spacing  $\Delta x = \frac{L_x}{I}$  and  $\Delta y = \frac{L_y}{J}$ . We then let

$$\begin{aligned} x_i &= (i + \frac{1}{2}) \Delta x, \quad i = 0, \dots, I - 1, \\ y_j &= (j + \frac{1}{2}) \Delta y, \quad j = 0, \dots, J - 1, \end{aligned}$$

and we define cell  $C_{i,j}$  to be

$$C_{i,j} = [x_{i-\frac{1}{2}}, x_{i+\frac{1}{2}}] \times [y_{j-\frac{1}{2}}, y_{j+\frac{1}{2}}],$$

where  $x_{i-\frac{1}{2}} = x_i - \frac{\Delta x}{2}$ , etc.

We approximate  $\rho$  by its average value over each cell using

$$\rho_{i,j}(t) \approx \frac{\int_{C_{i,j}} \rho(x, t) \sqrt{|G|} dx}{\int_{C_{i,j}} \sqrt{|G|} dx},$$

and we let  $\rho_{i,j}^n \approx \rho_{i,j}(n\Delta t)$ , where  $\Delta t$  is the time step.

The presence of off-diagonal terms in  $G^{-1}$  introduces tradeoffs in the construction of a discretization. In particular, a standard finite volume discretization of the Laplace-Beltrami operator results in a semi-discrete system that fails to satisfy the fluctuation dissipation balance. Here we construct a discretization that satisfies a discrete fluctuation dissipation balance. We first define a discrete gradient by

$$\nabla_h^- \rho_{i,j} := \begin{pmatrix} \frac{\rho_{i,j} - \rho_{i-1,j}}{\Delta x} \\ \frac{\rho_{i,j} - \rho_{i,j-1}}{\Delta y} \end{pmatrix}.$$

We next define the discrete divergence operator,  $\nabla_h^+ \cdot$ , acting on a discrete vector field,  $(u_{i,j}, v_{i,j})^T$ , by taking the discrete adjoint of  $\nabla_h^-$  to obtain

$$\nabla_h^+ \cdot \begin{pmatrix} u_{i,j} \\ v_{i,j} \end{pmatrix} := \frac{u_{i+1,j} - u_{i,j}}{\Delta x} + \frac{v_{i,j+1} - v_{i,j}}{\Delta y}.$$

Using these definitions, we obtain the semi-discrete system of stochastic ODEs

$$\begin{aligned} d\rho_{i,j} = & \frac{1}{\sqrt{|G|_{i,j}}} \nabla_h^+ \cdot (\sqrt{|G|_{i,j}} G_{i,j}^{-1} \nabla_h^- \rho_{i,j}) dt + \frac{1}{\sqrt{|G|_{i,j}}} \nabla_h^+ \cdot (\sqrt{|G|_{i,j}} \rho_{i,j} G_{i,j}^{-1} \nabla_h^- V_{i,j}) dt \\ & + \sqrt{\frac{2}{N}} \frac{1}{\sqrt{|G|_{i,j}}} \nabla_h^+ \cdot \left( \sqrt{\rho_{i,j}} |G|_{i,j}^{1/4} G_{i,j}^{-1/2} \frac{1}{\sqrt{\Delta x \Delta y}} \begin{pmatrix} dW_{i,j}^x \\ dW_{i,j}^y \end{pmatrix} \right), \end{aligned} \quad (33)$$

where the  $(W_{i,j}^{x,y})_{i,j,x,y}$  are a collection of independent standard two-dimensional Brownian motions. In this discretization, all terms involving the metric tensor,  $G$ , and the potential,  $V$ , are evaluated at the cell center using analytic formulae. We note that  $G_{i,j}^{-1/2}$  is not uniquely defined. Any choice of  $G_{i,j}^{-1/2}$  that satisfies  $G_{i,j}^{-1/2} (G_{i,j}^{-1/2})^T = G_{i,j}^{-1}$  will yield the same behavior.

The semidiscrete system Eq. (33) with  $V \equiv 0$  can be written in matrix form as

$$\begin{aligned} d\rho = & \mathbf{J}^{-1} \nabla_h^+ \mathbf{J} \mathbf{G}^{-1} \nabla_h^- \rho dt \\ & + \sqrt{\frac{2}{N \Delta x \Delta y}} \mathbf{J}^{-1} \nabla_h^+ \left( \text{Diag}(\sqrt{\rho}) \mathbf{J}^{1/2} \mathbf{G}^{-1/2} \begin{pmatrix} d\mathbf{W}^x \\ d\mathbf{W}^y \end{pmatrix} \right), \end{aligned} \quad (34)$$

where  $\rho = (\rho_{i,j})$  and  $\mathbf{W}^x, \mathbf{W}^y$  are independent  $IJ$ -dimensional Brownian motions,  $\mathbf{J}$  is an  $IJ \times IJ$  diagonal matrix of  $\sqrt{|G|}$ , and  $\nabla_h^+$  is  $IJ \times 2IJ$  matrix that represents the discrete gradient and  $\nabla_h^-$  is the  $2IJ \times IJ$  matrix that represents the discrete divergence.  $\text{Diag}(\alpha)$  is a  $2IJ \times 2IJ$  diagonal matrix formed from  $2 \times 2$  blocks of the form

$$\begin{pmatrix} \alpha_{i,j} & 0 \\ 0 & \alpha_{i,j} \end{pmatrix}.$$

Finally,  $\mathbf{G}^{-1}$  and  $\mathbf{G}^{-1/2}$  are block diagonal  $2IJ \times 2IJ$  matrices where the blocks are the  $2 \times 2$  matrices  $G_{i,j}^{-1}$  and  $G_{i,j}^{-1/2}$ , respectively.

To derive the fluctuation-dissipation relation, we now consider the system linearized around the time-stationary mean-field limit  $\bar{\rho} = \frac{1}{\nu(D)}$ , which can be written as

$$d\mathbf{Z} = \mathbf{J}^{-1} \mathbf{L}_h \mathbf{Z} dt + \sqrt{\frac{2\bar{\rho}}{N \Delta x \Delta y}} \mathbf{J}^{-1} \mathbf{K}_h \begin{pmatrix} d\mathbf{W}^x \\ d\mathbf{W}^y \end{pmatrix}, \quad (35)$$

where

$$\mathbf{L}_h = \nabla_h^+ (\mathbf{J} \mathbf{G}^{-1} \nabla_h^-) \quad \text{and} \quad \mathbf{K}_h = \nabla_h^+ \mathbf{J}^{1/2} \mathbf{G}^{-1/2}.$$

The stationary covariance of  $\mathbf{Z}$ , denoted by  $C_{\mathbf{Z}}$  is then given by

$$\mathbf{J}^{-1} \mathbf{L}_h C_{\mathbf{Z}} + C_{\mathbf{Z}} \mathbf{L}_h^* \mathbf{J}^{-1} = -\frac{2\bar{\rho}}{N \Delta x \Delta y} \mathbf{J}^{-1} \mathbf{K}_h \mathbf{K}_h^* \mathbf{J}^{-1}.$$

In the construction of the discretization,  $\nabla_h^+ \cdot$  and  $\nabla_h^-$  are adjoint with

$$\mathbf{L}_h = \mathbf{L}_h^* = -\mathbf{K}_h \mathbf{K}_h^*,$$

so that

$$C_{\mathbf{Z}} = \frac{\bar{\rho}}{N \Delta x \Delta y} \mathbf{J}^{-1}. \quad (36)$$

Equation (36) shows the fluctuation dissipation relation for the spatially discrete system in coordinate space. This result is consistent with the fluctuation dissipation result (24) discussed for the linearized SPDE, which implies that the numerical method will generate the correct equilibrium statistics.

We now consider the temporal discretization of Equation (33), assuming the metric tensor and the external potential do not depend on time. For simplicity we will only consider an Euler–Maruyama discretization to avoid complications associated with higher order temporal discretization of stochastic differential equations with multiplicative noise. This then gives the final discrete form

$$\begin{aligned} \rho_{i,j}^{n+1} = & \rho_{i,j}^n + \Delta t \left[ \frac{1}{\sqrt{|G|}_{i,j}} \nabla_h^+ \cdot (\sqrt{|G|}_{i,j} G_{i,j}^{-1} \nabla_h^- \rho_{i,j}^n) + \frac{1}{\sqrt{|G|}_{i,j}} \nabla_h^+ \cdot (\sqrt{|G|}_{i,j} \rho_{i,j}^n G_{i,j}^{-1} \nabla_h^- V_{i,j}) \right. \\ & \left. + \sqrt{\frac{2}{N}} \frac{1}{\sqrt{|G|}_{i,j}} \nabla_h^+ \cdot \left( \sqrt{\rho_{i,j}^n} |G|_{i,j}^{1/4} G_{i,j}^{-1/2} \frac{1}{\sqrt{\Delta t \Delta x \Delta y}} \begin{pmatrix} Z_{i,j}^x \\ Z_{i,j}^y \end{pmatrix} \right) \right], \end{aligned} \quad (37)$$

where the  $Z_{i,j}^{x,y}$  are centered normally distributed random numbers with

$$\mathbb{E}[Z_{i,j}^\alpha, Z_{i',j'}^{\alpha'}] = \delta_{i,i'} \delta_{j,j'} \delta_{\alpha,\alpha'},$$

for Kronecker deltas  $\delta$ .

## 5 Numerical experiments

In this section we present several computational examples demonstrating the behavior of the surface Dean–Kawasaki equation.

### 5.1 Equilibrium test

The first numerical example investigates the equilibrium statistical properties of the discretized system. For this case we consider the surface defined by

$$H(x, y) = a \sin(x) \sin(y).$$

The explicit formulae for the metric terms are given in Appendix A.

We discretize the system on  $[0, 2\pi]^2$  with  $a = 3$  on a  $32 \times 32$  grid and set the time step to  $\Delta t = 1.506 \times 10^{-4}$ , which is  $1.5625 \times 10^{-2}$  time the maximum stable time step for the discretization. The small time step minimizes errors associated with the Euler–Maruyama scheme.

We set the total number of particles to  $N = 10240$  and initialize

$$\rho = \frac{1}{\int_D \sqrt{|G|} dx},$$

which corresponds to the steady state solution of the system without noise. Here the integral is computed by summing  $\Delta x \Delta y \sqrt{|G|}$  over the grid. The system is evolved for  $10^5$  time steps to reach equilibrium. We then run for an additional  $10^6$  steps, gathering statistics every 10 steps. For comparison purposes, we also integrate the particle system given by (7) for the same length of time using the same time step, again with Euler–Maruyama. For the particle integration, we initialize the system with 10 particles per cell so that both systems have the same number of particles. We note that the particle initialization is not the same as the SPDE initialization; however, these differences have disappeared before we begin collecting statistics.

We consider two different representations of the data, one in terms of  $\rho$  and the other in terms of the number of particles in each cell, which we denote as  $N_{i,j}$ . To map between these representations, we note that

$$N_{i,j} = N \rho_{i,j} \sqrt{|G|} \Delta x \Delta y. \quad (38)$$

In Figure 1 we plot the mean values obtained from finite volume and particles simulations. The data is plotted in terms of number of particles per cell in Figure 2. The mean values of  $\rho$  on the grid are converging to the theoretical value  $\frac{1}{\int_D \sqrt{|G|} dx}$ . The mean values of  $N_{i,j}$  reflect the underlying structure of the surface as expected. More precisely, the average number of particles per cell is proportional to the area of the surface in that cell. As seen in Figure 2 both the finite volume method and the particle method recover the correct mean distribution.

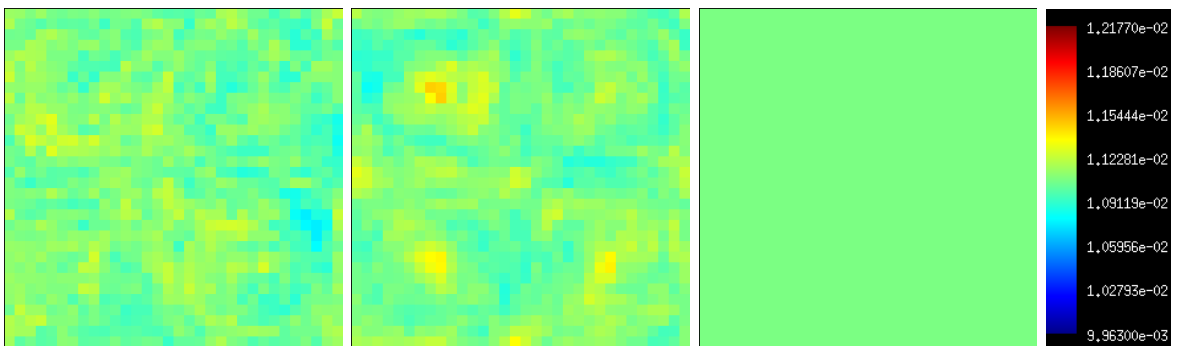


Figure 1: Mean of  $\rho$ . The left panel is the finite volume scheme, the middle panel is a Brownian particles simulation and the right panel is the theoretical result. Note that we have set the range to correspond to the theoretical mean  $\pm 10\%$ .

Next we consider the variance of the equilibrium distributions computed from the simulations. Although the mean value of  $\rho$  is constant over the domain, the variance of  $\rho$  is not.

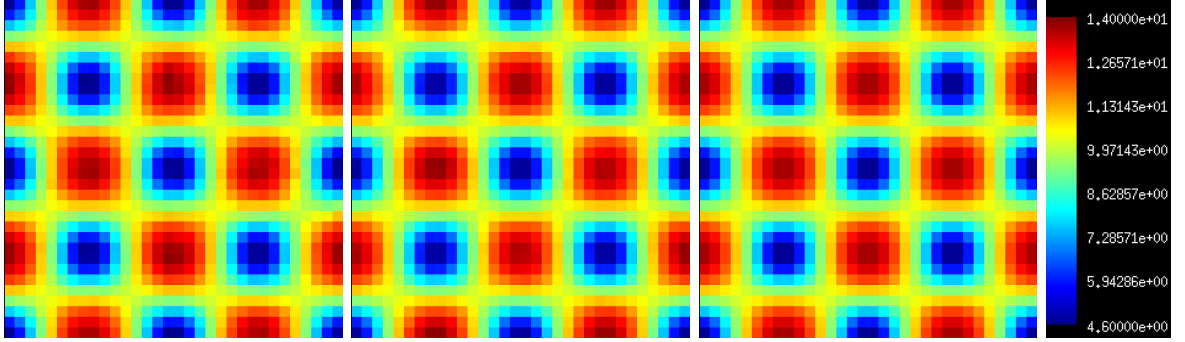


Figure 2: Mean number of particles in each cell. The left panel is the finite volume scheme, the middle panel is a Brownian particles simulation and the right panel is the theoretical result.

In particular, as discussed above in Equation (36),

$$\text{Var}(\rho_{i,j}) = \frac{1}{N A_S \sqrt{|G|_{i,j}} \Delta x \Delta y}$$

where  $A_S = \int_D \sqrt{|G|} dx$  is the surface area. This reflects the intuition that  $\rho$  has higher variability in cells where the local surface area is smaller. The variances of  $\rho$  obtained from the simulations are shown in Figure 3. Again, both the finite volume and particle data are in good agreement with the theoretical values.

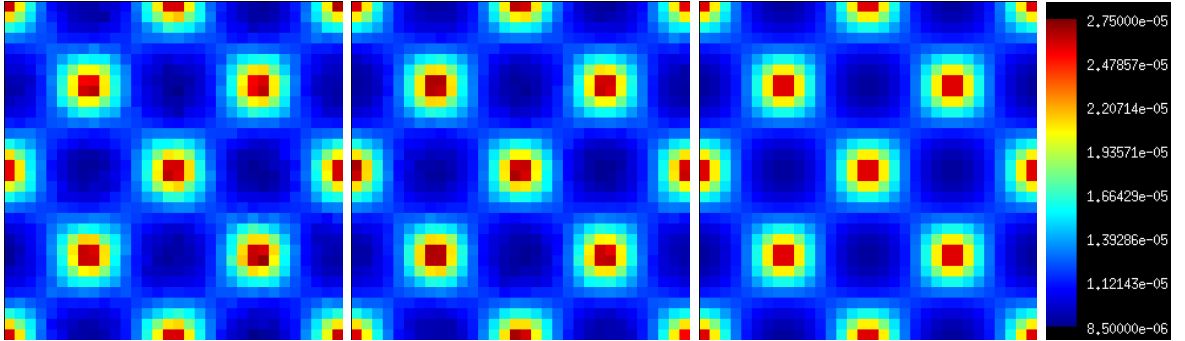


Figure 3: Variance of  $\rho$ . The left panel is the finite volume scheme, the middle panel is a Brownian particles simulation and the right panel is the theoretical result.

The variance of  $N_{i,j}$  is shown in Figure 4. The expected variance of  $N_{i,j}$  is given by

$$\text{Var}(N_{i,j}) = \frac{N \sqrt{|G|_{i,j}} \Delta x \Delta y}{A_S}.$$

When expressed in terms of number density there is more variability in regions with higher local surface area, which is the opposite of what was observed for the variance of  $\rho$ . Again, the figures show excellent agreement between the two simulations and the theoretical result. We also note that in the simulations  $\text{Var}(N_{i,j}) \approx \bar{N}_{i,j}$ . This reflects the underlying Poisson character of the particle equilibrium distribution. In particular, we expect the distribution of

particles within each cell to be Poisson distributed with a mean and variance proportional to the local surface area in that cell.

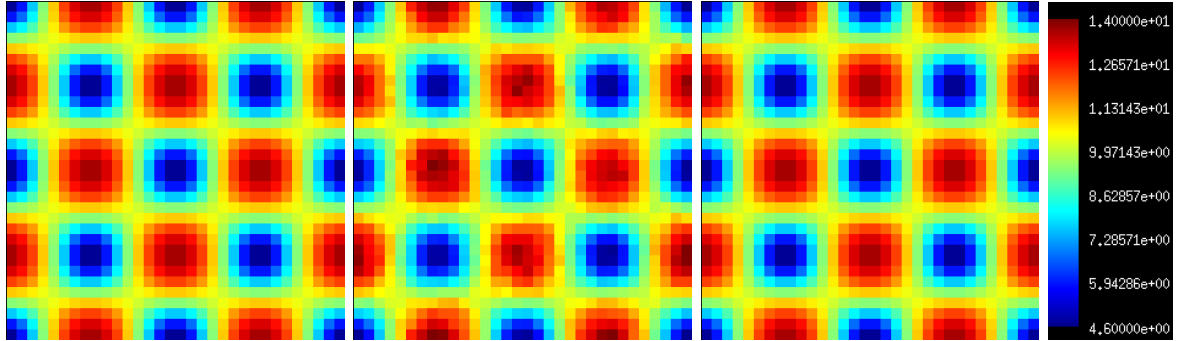


Figure 4: The variance of the number of particles in each cell. The left panel is the finite volume scheme, the middle panel is a Brownian particles simulation and the right panel is the theoretical result.

## 5.2 Transient simulations

In this section we illustrate the transient behavior of the surface Dean–Kawasaki equation. For the example presented here, the surface is given by

$$H(x, y) = 4 \sin^2(x) \sin^2(y).$$

The explicit formulae for the metric terms are given in Appendix B.

We discretize the system on  $[0, 2\pi) \times [0, 2\pi)$  on a  $64 \times 64$  grid and again we set the time step to  $\Delta t = 1.506 \times 10^{-4}$  which is  $1.5625 \times 10^{-2}$  time the maximum stable time step for the discretization. The small time step minimizes errors associated with the Euler–Maruyama scheme.

We set the total number of particles to  $N = 100000$  and initialize

$$\rho_{i,j} = \begin{cases} 0.801421 & \text{if } \sqrt{(x_{i,j} - \pi)^2 + (y_{i,j} - \pi)^2} < 0.2\pi \\ 0 & \text{otherwise} \end{cases},$$

which satisfies  $\int_D \rho(x) dx = 1$ . The surface consists of four peaks of height 4 at

$$(\pi \pm \pi/2, \pi \pm \pi/2)$$

and the initial condition is nonzero in a small circle between the four peaks.

The simulation was run for 50,000 time steps. Figure 5 shows a time sequence of the solution plotted on the surface. In the image, we have reduced height of the peaks so that  $\rho$  is not obscured. Also, we have set the range of  $\rho$  to be the same for all the images. The peak of  $\rho$  is initially around 0.8 but decays rapidly over time. Consequently the central red region of the images at early time are over saturated. Eventually,  $\rho$  would evolve to reach a constant value over the entire domain. However, at early times  $\rho$  diffuses more slowly into steep regions where the local area is large. This can be seen in the images where  $\rho$  is rapidly diffusing through the valleys and more slowly diffusing up the steep parts of the surface.

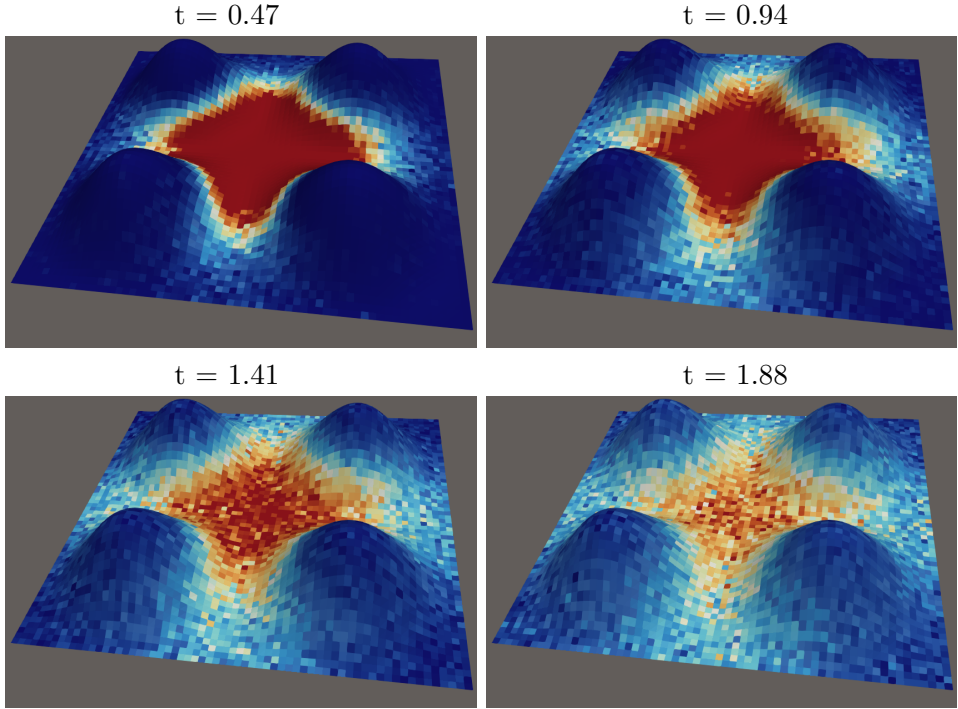


Figure 5: Time evolution of  $\rho$ . The range of  $\rho$  in the image is restricted to  $[0, 0.4]$  so the values are clipped particularly at early times. The peak values of  $\rho$ , left to right, are 0.166, 0.0786, 0.0542 and 0.0457. The height of the peaks on the surface have been scaled by 0.3 so that  $\rho$  is not obscured.

In Figure 6 we present the results of the same simulation expressed in terms of number of particles per cell,  $N_{i,j}$ . As we did before, we have set the range of  $N_{i,j}$  to be the same for all images, which results in clipping of the values particularly at early times. The key observation in these images is that the diffusive process is slowed in regions where the surface is steep, and the number of particles in those regions is quite high. This reflects the notion that we expect more particles to be present in cells with higher local surface area. Consequently, as the particles diffuse through the domain we observe high number of particles in the steep regions of the peaks and the center of the domain.

### 5.3 Effect of an external potential

In this section, we present results for same surface as was used in Section 5.2; however, now we introduce an external potential. Specifically, we set

$$V(x, y) = 5 \sin^2(x) \sin^2(y).$$

Although the potential is of the same form as the surface, the effect of the potential on the dynamics is quite different. From the perspective of the original particles dynamics, a steep region of the surface slows the particles motion relative to the  $(x, y)$  coordinate system, whereas a steep region in the potential biases the particle motion to move downhill to a lower value of the potential.

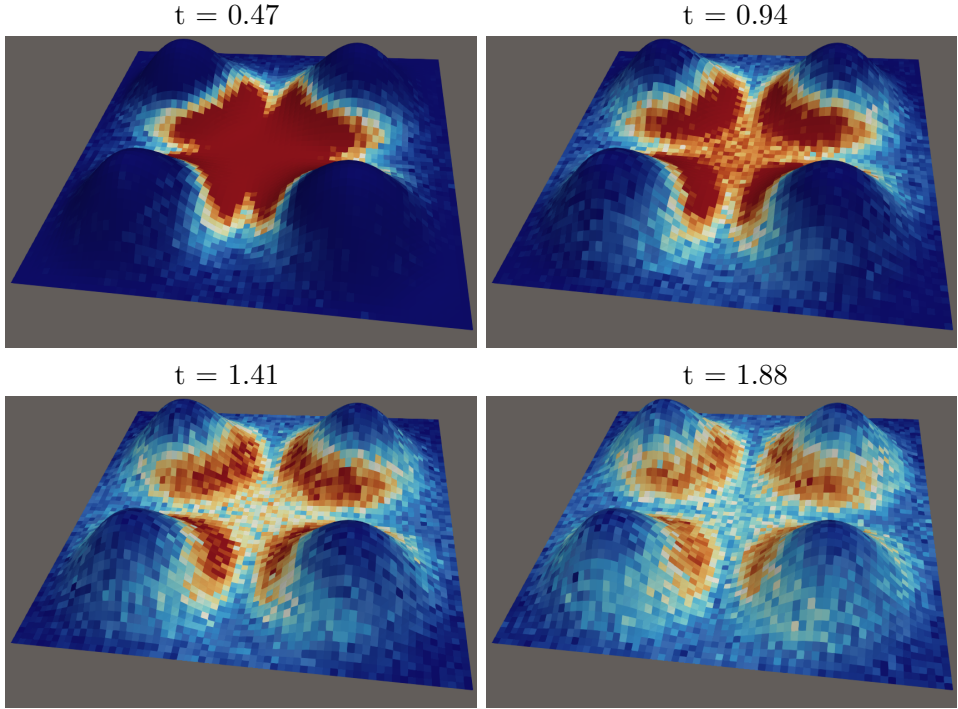


Figure 6: Time evolution of  $N_{i,j}$ . The range of  $N_{i,j}$  in the image is restricted to  $[0, 80]$  so the values are clipped particularly at early times. The peak values of  $N_{i,j}$ , left to right are 177, 135, 103 and 81. As in Figure 5 height of the peaks on the surface have been scaled by 0.3 so that the solution is not obscured.

This type of behavior is illustrated in Figure 7. The simulation parameters and the initial conditions are the same as in Section 5.2. For comparison purposes, we have used the same scaling here as in Figure 5. As seen in the images,  $\rho$  is more localized in the valleys of the surface, which also corresponds to the minimum of the potential surface. The presence of the potential suppresses  $\rho$  diffusing up the peaks and leads to higher peak values of the solution. The focusing effect of the potential also results in higher values of  $\rho$  reaching the boundary and one begins to see the solution diffusing around the outer portion of the peaks.

Figure 8 shows the results of the simulation with an external potential expressed in terms of number of particles per cell. As with  $\rho$  the potential leads to a concentration of  $N_{i,j}$  in the lower potential regions of the domain. The most striking feature of images is that the potential suppresses the high concentration of particles on the steep inner part of the surface. The two-pronged structure where the solution is diffusing down the channel between the peaks reflects the tradeoff between the tendency to have more particles in regions where the surface is steeper and the impact of the potential on biasing the particles toward the low potential region in the center of the channel.

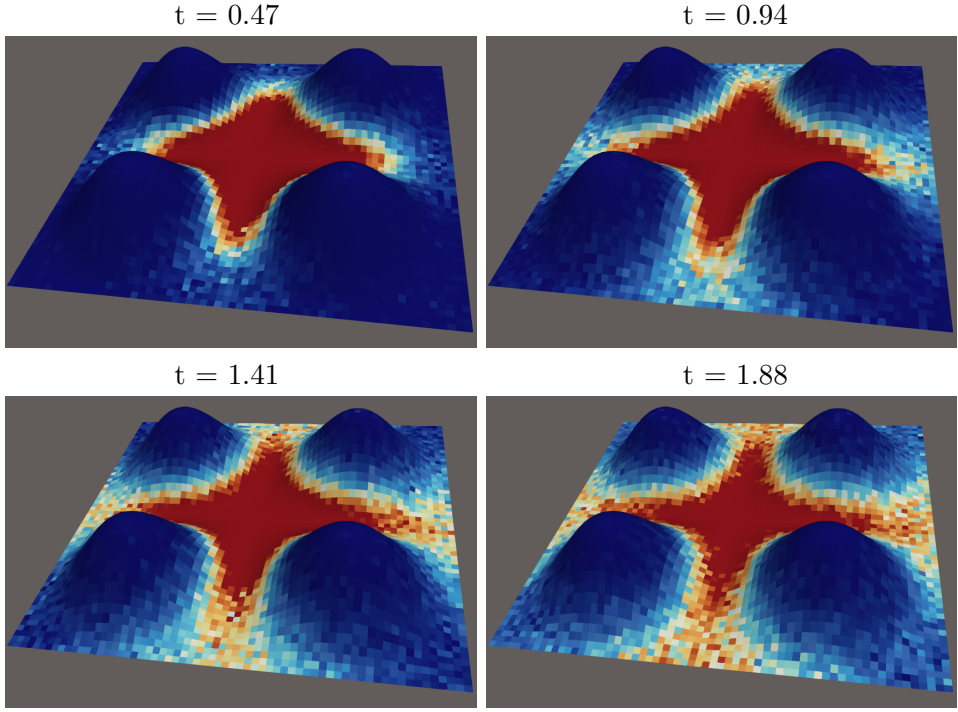


Figure 7: Time evolution of  $\rho$  with an external potential. The range of  $\rho$  in the image is restricted to  $[0, 0.4]$  so the values are clipped particularly at early times. The peak values of  $\rho$ , left to right are 0.203, 0.125, 0.0957 and 0.0856. As before, the height of the peaks on the surface have been scaled by 0.3 so that  $\rho$  is not obscured.

## Appendix A Sinusoidal perturbation of a square

In order to avoid leaving the patch problem, we consider perturbed square with periodic identification:  $(x, y) \in [0, 2\pi]^2$ . The sinusoidal perturbation of a square is given by

$$H(x, y) = a \sin(x) \sin(y),$$

where  $a$  is some positive constant.

We can compute all the geometric quantities explicitly: First note that

$$\begin{aligned} \nabla H(x, y) &= (a \cos x \sin y, a \sin x \cos y), \\ G(x, y) &= \begin{pmatrix} 1 + a^2 \cos^2 x \sin^2 y & a^2 \cos x \sin x \sin y \cos y \\ a^2 \cos x \sin x \sin y \cos y & 1 + a^2 \sin^2 x \cos^2 y \end{pmatrix} \\ &= \begin{pmatrix} 1 + p^2 & pq \\ pq & 1 + q^2 \end{pmatrix}, \end{aligned}$$

where  $p = a \cos x \sin y$  and  $q = a \sin x \cos y$ . We then have

$$|G(x, y)| = 1 + p^2 + q^2 =: s(x, y),$$

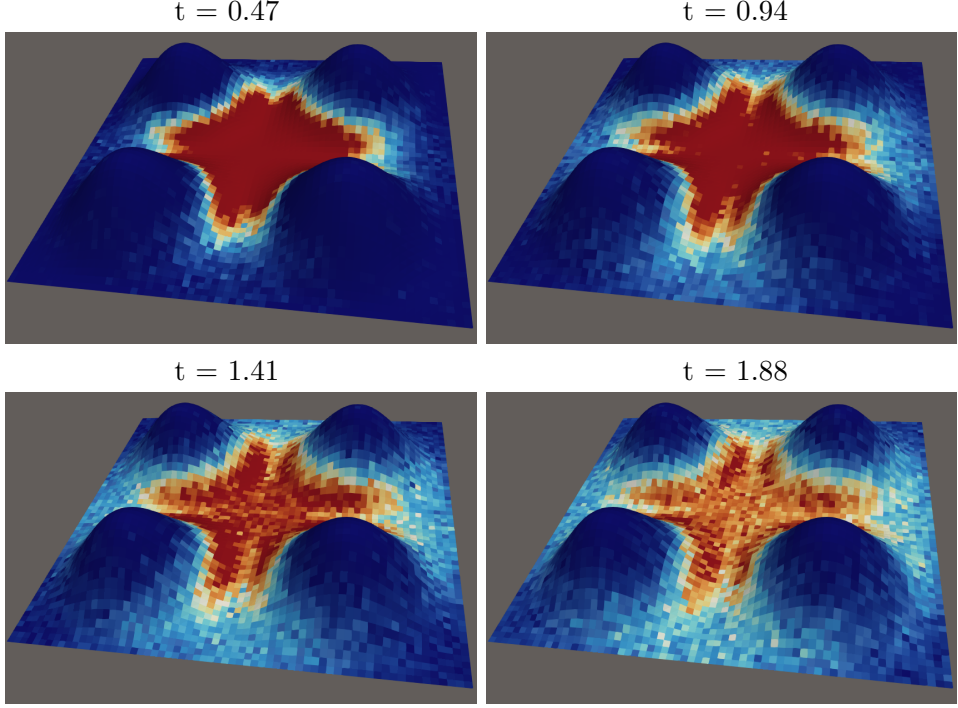


Figure 8: Time evolution of  $N_{i,j}$  with an external potential. The range of  $N_{i,j}$  in the image is restricted to  $[0, 80]$  so the values are clipped particularly at early times. The peak values of  $N_{i,j}$ , left to right are 196, 144, 123 and 109. As before, the height of the peaks on the surface have been scaled by 0.3 so that the solution is not obscured.

and

$$G^{-1} = \begin{pmatrix} 1+q^2 & -pq \\ \frac{s}{s} & \frac{1+p^2}{s} \\ -\frac{pq}{s} & \frac{1+p^2}{s} \end{pmatrix} \quad \text{and} \quad G^{-1/2} = \begin{pmatrix} 1-cp^2 & -cpq \\ -cpq & 1-cq^2 \end{pmatrix},$$

where

$$c = \frac{1}{s + \sqrt{s}}.$$

We note that  $G^{-1/2}$  is not unique; however, as long as  $G^{-1/2}(G^{-1/2})^T = G^{-1}$ , the noise term will have the correct covariance.

Finally, for particle simulations we need to evaluate

$$b \begin{pmatrix} x \\ y \end{pmatrix} = \frac{1}{\sqrt{|G|}} \nabla \cdot \left( \sqrt{|G|} G^{-1} \right) \begin{pmatrix} x \\ y \end{pmatrix}$$

in Equation (7):

$$b^x = \frac{a^2(2 + a^2(\cos^2 x + \cos^2 y)) \sin x \cos x \sin^2 y}{s^2}, \quad (39)$$

$$b^y = \frac{a^2(2 + a^2(\cos^2 x + \cos^2 y)) \sin y \cos y \sin^2 x}{s^2}. \quad (40)$$

## Appendix B Four peak surface

The second surface we consider features four peaks on the domain  $(x, y) \in [0, 2\pi)^2$ . The surface in this case is given by

$$H(x, y) = a \sin^2(x) \sin^2(y)$$

where  $a$  is some positive constant.

All the geometric quantities can be compute explicitly as:

$$\begin{aligned} \nabla H(x, y) &= \begin{pmatrix} 2a \cos x \sin x \sin^2 y \\ 2a \sin^2 x \cos y \sin y \end{pmatrix}, \\ G(x, y) &= \begin{pmatrix} 1 + 4a^2 \cos^2 x \sin^2 x \sin^4 y & 4a^2 \cos x \sin^3 x \sin^3 y \cos y \\ 4a^2 \cos x \sin^3 x \sin^3 y \cos y & 1 + 4a^2 \sin^4 x \cos^2 y \sin^2 y \end{pmatrix}. \\ &= \begin{pmatrix} 1 + p^2 & pq \\ pq & 1 + q^2 \end{pmatrix}, \end{aligned}$$

where  $p = 2a \cos x \sin x \sin^2 y$  and  $q = 2a \sin^2 x \cos y \sin y$ . We then have

$$|G(x, y)| = 1 + p^2 + q^2 =: s(x, y),$$

and

$$G^{-1} = \begin{pmatrix} \frac{1+q^2}{s} & -\frac{pq}{s} \\ -\frac{pq}{s} & \frac{1+p^2}{s} \end{pmatrix} \quad \text{and} \quad G^{-1/2} = \begin{pmatrix} 1 - cp^2 & -cpq \\ -cpq & 1 - cq^2 \end{pmatrix},$$

where

$$c = \frac{1}{s + \sqrt{s}}.$$

We again note that  $G^{-1/2}$  is not unique; however, as long as  $G^{-1/2}(G^{-1/2})^T = G^{-1}$ , the noise term will have the correct covariance.

Finally, for particle simulations we need to evaluate

$$b \begin{pmatrix} x \\ y \end{pmatrix} = \frac{1}{\sqrt{|G|}} \nabla \cdot \left( \sqrt{|G|} G^{-1} \right) \begin{pmatrix} x \\ y \end{pmatrix}$$

in Equation (7). We first compute the derivatives of  $s$  with respect to  $x$  and  $y$  to obtain

$$\begin{aligned} s_x &= 8a^2 \sin x \sin y \cos x (2 \cos^2 y \sin^2 x \sin y + \sin^3 y (\cos^2 x - \sin^2 x)) \\ s_y &= 8a^2 \sin x \sin y \cos y (2 \cos^2 x \sin^2 y \sin x + \sin^3 x (\cos^2 y - \sin^2 y)). \end{aligned}$$

We then have

$$\begin{aligned} b^x &= 2a^2 \left( \frac{2 \cos x \sin^3 x \sin^2 y}{s} + \frac{[\cos x \cos y \sin^3 x \sin^3 y] s_y}{s^2} \right) - \frac{[4a^2 \cos^2 y \sin^3 x \sin^3 y + 1] s_x}{2s^2} \\ b^y &= 2a^2 \left( \frac{2 \cos y \sin^3 y \sin^2 x}{s} + \frac{[\cos x \cos y \sin^3 x \sin^3 y] s_x}{s^2} \right) - \frac{[4a^2 \cos^2 x \sin^3 x \sin^3 y + 1] s_y}{2s^2}. \end{aligned}$$

## Appendix C Additional proofs

*Proof of Lemma 9.* By a monotone class argument, it suffices to show that

$$\mathbb{E}[(M_t - M_s)F_s\Phi(B)] = 0$$

for all  $0 \leq s \leq t$  and all bounded and  $\mathcal{F}_s$ -measurable  $F_s$  and all bounded measurable  $\Phi : C(\mathbb{R}_+, \mathbb{R}^d) \rightarrow \mathbb{R}$ . By the martingale representation theorem for  $B$ , there exists a square-integrable adapted  $H$  with

$$\Phi(B) = \mathbb{E}[\Phi(B)] + \int_0^\infty H_r \cdot dB_r,$$

hence

$$\begin{aligned} \mathbb{E}[(M_t - M_s)F_s\Phi(B)] &= \mathbb{E}\left[(M_t - M_s)F_s\left(\mathbb{E}[\Phi(B)] + \int_0^s H_r \cdot dB_r\right)\right] \\ &\quad + \mathbb{E}\left[(M_t - M_s)F_s \int_s^\infty H_r \cdot dB_r\right] \\ &= 0, \end{aligned}$$

where we used the tower property to insert  $\mathbb{E}[\cdot | \mathcal{F}_s]$  for both terms, and for the second term we also used that the product of  $M$  with the stochastic integral is a martingale, because

$$\begin{aligned} (M_{\cdot \wedge t} - M_s) \int_s^\cdot H_r \cdot dB_r &= (M_{\cdot \wedge t} - M_s) \int_s^\cdot H_r \cdot dB_r - \int_s^{\cdot \wedge t} H_r \cdot d\langle M, B \rangle_r \\ &= (M_{\cdot \wedge t} - M_s) \int_s^\cdot H_r \cdot dB_r - \left\langle (M_{\cdot \wedge t} - M_s), \int_s^\cdot H_r \cdot dB_r \right\rangle. \end{aligned}$$

□

## Acknowledgment

The authors are grateful to Ann Almgren for her help with numerical experiments and Mirjana Djorić for informative discussions about the geometric setting. ADj and NP gratefully acknowledge funding by Deutsche Forschungsgemeinschaft (DFG) through grant CRC 1114 “Scaling Cascades in Complex Systems”, Project Number 235221301, Project C10 “Numerical Analysis for nonlinear SPDE models of particle systems”. This material is based upon work supported by the National Science Foundation under Grant No. DMS-2424139, while ADj and NP were in residence at the Simons Laufer Mathematical Sciences Institute in Berkeley, California, during the Fall 2025 semester. Further support of ADj is by Daimler and Benz Foundation as part of the scholarship program for junior professors and postdoctoral researchers. The work of JB was supported by the U.S. Department of Energy, Office of Science, Office of Advanced Scientific Computing Research, Applied Mathematics Program under contract No. DE-AC02-05CH11231.

## References

[1] Paul C Bressloff and Jay M Newby. Stochastic models of intracellular transport. *Reviews of Modern Physics*, 85(1):135–196, 2013.

- [2] Pavel Castro-Villarreal. Brownian motion meets riemann curvature. *Journal of Statistical Mechanics: Theory and Experiment*, 2010(08):P08006, 2010.
- [3] Sun-Ho Choi, Dohyun Kwon, and Hyowon Seo. Multi-agent system for target tracking on a sphere and its asymptotic behavior. *Communications in Nonlinear Science and Numerical Simulation*, 117:106967, 2023.
- [4] Giovanni Ciccotti, Tony Lelievre, and Eric Vanden-Eijnden. Projection of diffusions on submanifolds: Application to mean force computation. *Communications on Pure and Applied Mathematics: A Journal Issued by the Courant Institute of Mathematical Sciences*, 61(3):371–408, 2008.
- [5] Federico Cornalba and Julian Fischer. The Dean-Kawasaki equation and the structure of density fluctuations in systems of diffusing particles. *Arch. Ration. Mech. Anal.*, 247(5):Paper No. 76, 59, 2023.
- [6] Federico Cornalba, Julian Fischer, Jonas Ingmanns, and Claudia Raithel. Density fluctuations in weakly interacting particle systems via the Dean-Kawasaki equation. *arXiv preprint arXiv:2303.00429*, 2023.
- [7] Giuseppe Da Prato and Jerzy Zabczyk. *Stochastic equations in infinite dimensions*, volume 152 of *Encyclopedia of Mathematics and its Applications*. Cambridge University Press, Cambridge, second edition, 2014.
- [8] David S Dean. Langevin equation for the density of a system of interacting Langevin processes. *Journal of Physics A: Mathematical and General*, 29(24):L613, 1996.
- [9] Ana Djurdjevac, Xiaohao Ji, and Nicolas Perkowski. Weak error of Dean-Kawasaki equation with smooth mean-field interactions. *arXiv preprint arXiv:2502.20929*, 2025.
- [10] Ana Djurdjevac, Helena Kremp, and Nicolas Perkowski. Weak error analysis for a nonlinear SPDE approximation of the Dean-Kawasaki equation. *Stoch. Partial Differ. Equ. Anal. Comput.*, 12(4):2330–2355, 2024.
- [11] Aleksandar Donev, Eric Vanden-Eijnden, Alejandro Garcia, and John Bell. On the accuracy of finite-volume schemes for fluctuating hydrodynamics. *Communications in Applied Mathematics and Computational Science*, 5(2):149–197, 2010.
- [12] Andrew B. Duncan, Charles M. Elliott, Grigoris A. Pavliotis, and Andrew M. Stuart. A multiscale analysis of diffusions on rapidly varying surfaces. *J. Nonlinear Sci.*, 25(2):389–449, 2015.
- [13] Weinan E, Tiejun Li, and Eric Vanden-Eijnden. *Applied stochastic analysis*, volume 199 of *Grad. Stud. Math.* Providence, RI: American Mathematical Society (AMS), 2019.
- [14] Benjamin Fehrman and Benjamin Gess. Non-equilibrium large deviations and parabolic-hyperbolic PDE with irregular drift. *Invent. Math.*, 234(2):573–636, 2023.
- [15] Benjamin Fehrman and Benjamin Gess. Well-posedness of the Dean-Kawasaki and the nonlinear Dawson-Watanabe equation with correlated noise. *Arch. Ration. Mech. Anal.*, 248(2):Paper No. 20, 60, 2024.

- [16] Massimo Fornasier, Hui Huang, Lorenzo Pareschi, and Philippe Sünnen. Consensus-based optimization on the sphere: convergence to global minimizers and machine learning. *J. Mach. Learn. Res.*, 22:Paper No. 237, 55, 2021.
- [17] Nir Gov. Membrane undulations driven by force fluctuations of active proteins. *Physical review letters*, 93(26):268104, 2004.
- [18] Luzie Helfmann, Nataša Djurdjevac Conrad, Ana Djurdjevac, Stefanie Winkelmann, and Christof Schütte. From interacting agents to density-based modeling with stochastic PDEs. *Commun. Appl. Math. Comput. Sci.*, 16(1):1–32, 2021.
- [19] Elton P. Hsu. *Stochastic analysis on manifolds*, volume 38 of *Graduate Studies in Mathematics*. American Mathematical Society, Providence, RI, 2002.
- [20] Kyozi Kawasaki. Stochastic model of slow dynamics in supercooled liquids and dense colloidal suspensions. *Physica A: Statistical Mechanics and its Applications*, 208(1):35–64, 1994.
- [21] Vitalii Konarovskiy, Tobias Lehmann, and Max von Renesse. On Dean–Kawasaki dynamics with smooth drift potential. *J. Stat. Phys.*, pages 1–16, 2020.
- [22] Vitalii Konarovskiy, Tobias Lehmann, and Max-K. von Renesse. Dean-Kawasaki dynamics: ill-posedness vs. triviality. *Electron. Commun. Probab.*, 24:Paper No. 8, 9, 2019.
- [23] Tony Lelièvre, Mathias Rousset, and Gabriel Stoltz. *Free energy computations. A mathematical perspective*. London: Imperial College Press, 2010.
- [24] Lawrence C-L Lin, Nir Gov, and Frank LH Brown. Nonequilibrium membrane fluctuations driven by active proteins. *The Journal of chemical physics*, 124(7), 2006.
- [25] Erik Lindahl and Mark SP Sansom. Membrane proteins: molecular dynamics simulations. *Current opinion in structural biology*, 18(4):425–431, 2008.
- [26] Reinhart Lipowsky and Erich Sackmann. *Structure and dynamics of membranes: I. from cells to vesicles/II. generic and specific interactions*. Elsevier, 1995.
- [27] Ali Naji and Frank LH Brown. Diffusion on ruffled membrane surfaces. *The Journal of chemical physics*, 126(23), 2007.
- [28] Ellen Reister and Udo Seifert. Lateral diffusion of a protein on a fluctuating membrane. *Europhysics Letters*, 71(5):859, 2005.
- [29] Ellen Reister-Gottfried, Stefan M Leitenberger, and Udo Seifert. Hybrid simulations of lateral diffusion in fluctuating membranes. *Physical Review E—Statistical, Nonlinear, and Soft Matter Physics*, 75(1):011908, 2007.
- [30] Ellen Reister-Gottfried, Stefan M Leitenberger, and Udo Seifert. Diffusing proteins on a fluctuating membrane: Analytical theory and simulations. *Physical Review E—Statistical, Nonlinear, and Soft Matter Physics*, 81(3):031903, 2010.
- [31] Michael J Saxton and Ken Jacobson. Single-particle tracking: applications to membrane dynamics. *Annual review of biophysics and biomolecular structure*, 26(1):373–399, 1997.

[32] Alexander Yu. Veretennikov. On strong solution and explicit formulas for solutions of stochastic integral equations. *Math. USSR Sb.*, 39:387–403, 1981.